Journal of Solid State Chemistry **168,** 514–523 (2002)
doi:10.1006/jssc.2002.9749

The First Mixed Valence Radical Cation Salts of BEDT-TTF with the Photochromic Metal Mononitrosyl Complexes $[RuNOX_5]^{2-}$ (*X*=Br, Cl) as Counterions

I. Yu. Shevyakova,* L. V. Zorina,† S. S. Khasanov,† L. I. Buravov,* V. A. Tkacheva,* R. P. Shibaeva,† E. B. Yagubskii,* and E. Canadell‡,[1]

*Institute of Problems of Chemical Physics, Russian Academy of Sciences, 142432 Chernogolovka, MD, Russia; †Institute of Solid State Physics, Russian Academy of Sciences,142432 Chernogolovka, MD, Russia; and ‡Institut de Ciència de Materials de Barcelona (CSIC), Campus de la U.A.B., E-08193 Bellaterra, Spain

Received January 8, 2002; in revised form March 21, 2002; accepted March 25, 2002

New bis(ethylenedithio)tetrathiafulvalene BEDT-TTF radical cation salts with the $[RuNOX_5]^{2-}$ (X = Br, Cl) anions have been synthesized. The crystal structures of κ-(BEDT-TTF)$_4$[RuNOBr$_5$]·C$_6$H$_5$CN (1): $a = 8.747(2)$, $b = 12.088(1)$, $c = 17.300(2)$ Å, $\alpha = 95.63(1)$, $\beta = 91.93(2)$, $\gamma = 94.79(2)^\circ$, $V = 1812.3(5)$ Å^3, $P\bar{1}$, $Z = 1$ and δ-(BEDT-TTF)$_4$[RuNOCl$_5$]$_{1.33}$ (2): $a = 6.721(1)$, $b = 15.016(2)$, $c = 35.386(3)$ Å, $\alpha = 92.804(8)$, $V = 3567.0(8)$ Å^3, $I2/c$, $Z = 2$ have been determined. Their electronic band structures and transport properties have been studied. The radical cation salts κ-(BEDT-TTF)$_4$[RuNOCl$_5$]·C$_6$H$_5$CN (3) and δ-(BEDT-TTF)$_4$[RuNOBr$_5$] (4) have also been found to exist and are isostructural to 1 and 2, respectively. Evidence for commensurate and incommensurate structural modulations was found for 2 and 4, respectively. The crystals of 1 and 3 are semiconductors while those of 2 and 4 exhibit an M–I transition at 50 and 80 K, respectively. © 2002 Elsevier Science (USA)

Key Words: **organic conductors; radical cation salts; mononitrosyls; X-ray and band structure.**

1. INTRODUCTION

In the last few years, an increased interest has been devoted to hybrid multifunctional materials combining different physical properties: conductivity (or superconductivity) and magnetism [1–4], magnetism (or conductivity) and nonlinear optical properties [5–8], magnetism and photochromism [9], etc. One of the main goals of our recent work in this direction has been the search for a possible interplay between conductivity and photochromism in molecular conductors by incorporating photochromic metal complex anions into the radical cation salts of typical organic π-donors. This can provoke a specific interaction among the conducting and photochromic groups in the same crystal and thus lead to the creation of a novel electronic system in which the properties of the anions are correlated cooperatively to the electron transport. In this context, we have recently studied radical cation salts of organic π-donors like BEDT-TTF (bis(ethylenedithio)tetrathiafulvalene), BEDO-TTF (bis(ethylenedioxy)tetrathiafulvalene), EDT-TTF (ethylenedithiotetrathiafulvalene), DOET (dioxanediyldithioethylenedithiotetrathiafulvalene), TTT (tetrathiotetracene) and TSeT (tetraselenotetracene) with the $[FeNO(CN)_5]^{2-}$ nitroprusside (NP) anion (10–16). The TTF (tetrathiafulvalene), BET-TTF (bisethylenethiotetrathiafulvalene), BEST (bis(ethylenedithio)tetraselenafulvalene) and BETS (bis(ethylenediseleno)tetrathiafulvalene) radical cation salts with NP anions are also known [17–20].

Metal mononitrosyl complexes, such as $Na_2[NP]\cdot 2H_2O$, have been found to possess extremely long-living electronic excited states which can be induced by irradiation with light in the 350–580 nm wavelength range under liquid nitrogen temperature [21–26]. Such complexes can be used as building blocks for the preparation of new molecular conductors. In this contribution, we would like to report on the synthesis, crystal and electronic structures as well as transport properties of new mixed valence BEDT-TTF radical cation salts with the photochromic metal mononitrosyl complexes $[RuNOX_5]^{2-}$ (X = Br, Cl) as counterions. The completely ionic radical cation salts with these anions, $(BETS)_2[RuNOBr_5]$ and $(BETS)_2[RuNOCl_5]$ have been previously obtained [20].

[1] To whom correspondence should be addressed. Fax: +34-93-580-57-29. E-mail: canadell@icmab.es.

0022-4596/02 $35.00

2. EXPERIMENTAL

2.1. Synthesis

The radical cation salts were synthesized on a platinum wire electrode by the standard electrochemical oxidation of the donor in an H-shaped cell under low constant current ($I = 0.4-1\ \mu A$). The crystallization times vary from 6 to 20 days, depending on the salt. The conditions for the synthesis of the radical salts are summarized in Table 1.

2.2. X-ray Crystal Structure Analysis

The single crystals were initially studied by the X-ray photomethod (rotation and Weissenberg photographs) and then the crystals of **1** and **2** were mounted on an Enraf Nonius CAD4 diffractometer. Unit-cell parameters and the orientation matrix were determined by a standard least-squares refinement (Enraf Nonius CAD4 software) of the setting angles of 25 automatically centered reflections. Data collection was performed by the ω-scan technique [$\lambda(MoK\alpha) = 0.71073$ Å, graphite monochromator] at room temperature. Numerical data corrections were applied for Lorenz, polarization and absorption (for the crystal **2**, by the program DIFABS in AREN) effects. Selected experimental parameters and crystal data are listed in Table 2. The structures were solved by direct methods using the AREN program [27], followed by a Fourier synthesis, and refined using the SHELXL-93 program [28]. All atoms except hydrogen were refined anisotropically.

2.3. Electrical Resistivity Measurements

The d.c. resistivity measurements over the range 4.2–300 K were performed by the standard four-probe method on the best developed face of several single crystals (in the *ab* plane) of each sample. In the case of crystal **3**, the d.c. measurement was performed along the *c*-axis since the *ab* plane was not enough developed. Contacts to the crystals were glued with a graphite paste using 10–20 μm diameter platinum wires.

2.4. Band Structure Calculations

The tight-binding band structure calculations were based upon the effective one-electron Hamiltonian of the extended Hückel method [29]. The off-diagonal matrix elements of the Hamiltonian were calculated according to the modified Wolfsberg–Helmholz formula [30]. All valence electrons were explicitly taken into account in the calculations and the basis set consisted of double-ζ Slater-type orbitals for C and S and single-ζ Slater-type orbitals for H. The exponents, contraction coefficients and atomic parameters for C, S and H were taken from previous work [31].

3. RESULTS AND DISCUSSION

The radical cation salts were obtained by electrochemical oxidation of a solution containing the neutral BEDT-TTF donor and the corresponding complex anion $[RuNOBr_5]^{2-}$ or $[RuNOCl_5]^{2-}$. To make these two anions soluble, we

TABLE 1
Conditions for the Synthesis and Conducting Properties of the Radical Cation Salts 1–4

Salt	Reagents	Solvent	T, °C	σ_{rt}[a], S cm^{-1}
(**1**) κ-(BEDT-TTF)$_4$[RuNOBr$_5$]·BN	BEDT-TTF (0.015 g) Cs_2[RuNOBr$_5$] (0.037 g) 18-crown-6-ether-6 (0.026 g)	BN[b] (20 ml) C_2H_5OH (2 ml)	10	1.2
(**2**) δ-(BEDT-TTF)$_4$[RuNOCl$_5$]$_{1.33}$ or (BEDT-TTF)$_3$[RuNOCl$_5$]	BEDT-TTF (0.015 g) K_2[RuNOCl$_5$] (0.0175) 18-crown-6-ether-6 (0.026 g) or BEDT-TTF (0.015 g) $(Bu_4N)_2$[RuNOCl$_5$] (0.037 g)	NB[c] (20 ml) C_2H_5OH (2 ml) BN or NB (20 ml)	25 25	14–16
(**3**) κ-(BEDT-TTF)$_4$[RuNOCl$_5$] · BN	BEDT-TTF (0.015 g) $(Bu_4N)_2$[RuNOCl$_5$] (0.037 g)	BN (20 ml)	10	3×10^{-3}[d]
(**4**) δ-(BEDT-TTF)$_4$[RuNOBr$_5$]$_x$ ($x \sim 1$)	BEDT-TTF (0.015 g) Cs_2[RuNOBr$_5$] (0.037 g) 18-crown-6-ether-6 (0.026 g)	BN or NB (20 ml) C_2H_5OH (2 ml)	18	12

[a] Measured in the *ab* plane.
[b] BN—benzonitrile, C_6H_5CN.
[c] NB—nitrobenzene, $C_6H_5NO_2$.
[d] Measured along the c^*-axis.

TABLE 2
Crystal Data and Structure Determination Details for the Radical Cation Salts κ-(BEDT-TTF)$_4$[RuNOBr$_5$] · C$_6$H$_5$CN (1) and δ-(BEDT-TTF)$_4$[RuNOCl$_5$]$_{1.33}$ (2)

	1	2
Chemical formula	$C_{47}H_{37}Br_5N_2ORuS_{32}$	$C_{40}H_{32}Cl_{6.65}N_{1.33}O_{1.33}Ru_{1.33}S_{32}$
Formula weight	2172.3	1948.7
a (Å)	8.747(2)	6.721(1)
b (Å)	12.088(1)	15.016(2)
c (Å)	17.300(2)	35.386(3)
α (deg)	95.63(1)	92.804(8)
β (deg)	91.93(2)	90
γ (deg)	94.79(2)	90
V (Å^3)	1812.4(5)	3567.0(8)
$d_{calc.}$ (g cm^{-3})	1.990	1.814
Space group	$P\bar{1}$	$I2/c$
Z	1	2
μ (cm^{-1})	39.34	15.10
$2\theta_{max}$ (deg)	50	40
Reflections collected	3662	2878
Independent reflections, $I > 2\sigma(I)$	3352	1466
$R_{av.}$	0.0208	0.0110
No. of variables	476	216
R	0.0445	0.0350
R_{wp}	0.0823	0.0934
S	1.135	1.113

have followed two different procedures. One involves the prior preparation of the tetrabutylammonium salt of the anion which is already soluble in the common organic solvents. The other starts from a suspension of an alkaline salt (K^+ or Cs^+) of the anion which is made soluble by addition of crown ether and ethyl alcohol. Radical cation salts grew as shiny, black, plate-like single crystals of different size. The electrocrystallization temperature has a critical effect on the composition of the salts (κ- or δ-phases, see Table 1), while the solvents and electrolytes used influence only the quality and size of the crystals.

3.1. κ-(BEDT-TTF)$_4$[RuNOBr$_5$] · BN (1) and κ-(BEDT-TTF)$_4$[RuNOCl$_5$] · BN (3)

A projection of the crystal structure of **1** along the *a*-direction is shown in Fig. 1a. The structure consists of radical cation layers parallel to the *ab* plane, alternating with layers of the $[RuNOBr_5]^{2-}$ anions and solvent molecules, benzonitrile (BN, C_6H_5CN). The octahedral non-symmetrical anions are located at inversion centers and the non-symmetrical molecules of BN occupy inversion centers too. The Ru–Br bond length *trans* to the nitrosyl group (2.457(9) Å) is shorter than the average *cis*-(Ru–Br) bond length of 2.522(1) Å. The Ru–N–O group is approximately linear, with an Ru–N–O bond angle of 180(4)° and a Ru–N bond distance of 1.76(2) Å. The values of the *cis*-(Ru–Br) and Ru–N bond lengths as well as the Ru–N–O angle are in good agreement with the corresponding values in $K_2[RuNOBr_5]$, 2.517(3), 1.724 (17) Å and 174.4(1.3)°, respectively (32). However, the *trans*-(Ru–Br) bond length seems to be shorter [2.511(3) Å in $K_2[RuNOBr_5]$] due to the statistical distribution of the *trans* Br and NO ligands.

The projection of the radical cation layer along the BEDT-TTF long molecular axis is shown in Fig. 1b. As in all κ-phase salts, the radical cation layer is formed by dimers of the BEDT-TTF donors oriented in a roughly orthogonal manner (the angle is about 81.06(7)°). The radical cation layers are build from two types of centrosymmetric dimers I–I$_i$ and II–II$_i$ with interplanar distances 3.71 and 3.46 Å, respectively. The dimers have different overlap modes (Fig. 2). It should be noted that there are a number of short cation–anion and cation–solvent contacts. Most of the contacts are associated with the cation radical II: S···Br 3.699 Å, C···Br 3.50, 3.61, 3.66, 3.71 Å, S···O 3.32 Å, C···O 3.21 Å (cation–anion) and S···C 3.50 Å, S···N 3.25 Å, C···N 3.25 Å (cation–solvent), whereas only two contacts S···Br 3.586 Å and C···Br 3.58 Å are associated with the radical cation I. It should be noted that there is some intrinsic disorder in the crystal **1**, related to the orientation disordering of the ethylenedithio groups of both BEDT-TTF at room temperature and to the random orientation of solvent molecules, C_6H_5CN.

The conductivity of **1** at room temperature is $\cong 1.2\,\Omega^{-1}\,cm^{-1}$ (Table 1). The temperature dependence of the normalized resistivity, measured in the *ab* plane of the crystals, which is parallel to the donor layers, is displayed in Fig. 3. The resistivity increases upon cooling the sample, indicating a semiconducting behavior. From a logarithmic plot of the resistivity, we can estimate an activation energy (E_a) of 0.04 eV.

The repeat unit of the BEDT-TTF layers contains four donors. Thus, as shown in Fig. 4, the calculated band structure for a donor layer of **1** contains four bands built from the highest occupied molecular orbital (HOMO) of the donors. As mentioned, the layers contain two different donor molecules although from both structural and electronic viewpoints these donors are quite similar (i.e., the difference in the central C—C bond lengths (1.363 (donor I) and 1.353 (donor II)) does not exceed 0.01 Å and the difference in energy of their HOMOs is only 0.03 eV). It is then surprising to see that the general shape of the band structure is quite different from that of the usual κ-phases [33]. The reason for that can be understood when looking at the strength of the different $\beta_{HOMO-HOMO}$ interaction energies [34] of Table 3. Whereas in the usual κ-phases, the strength of the HOMO···HOMO interaction for the two dimeric units is the same (when imposed by symmetry) or

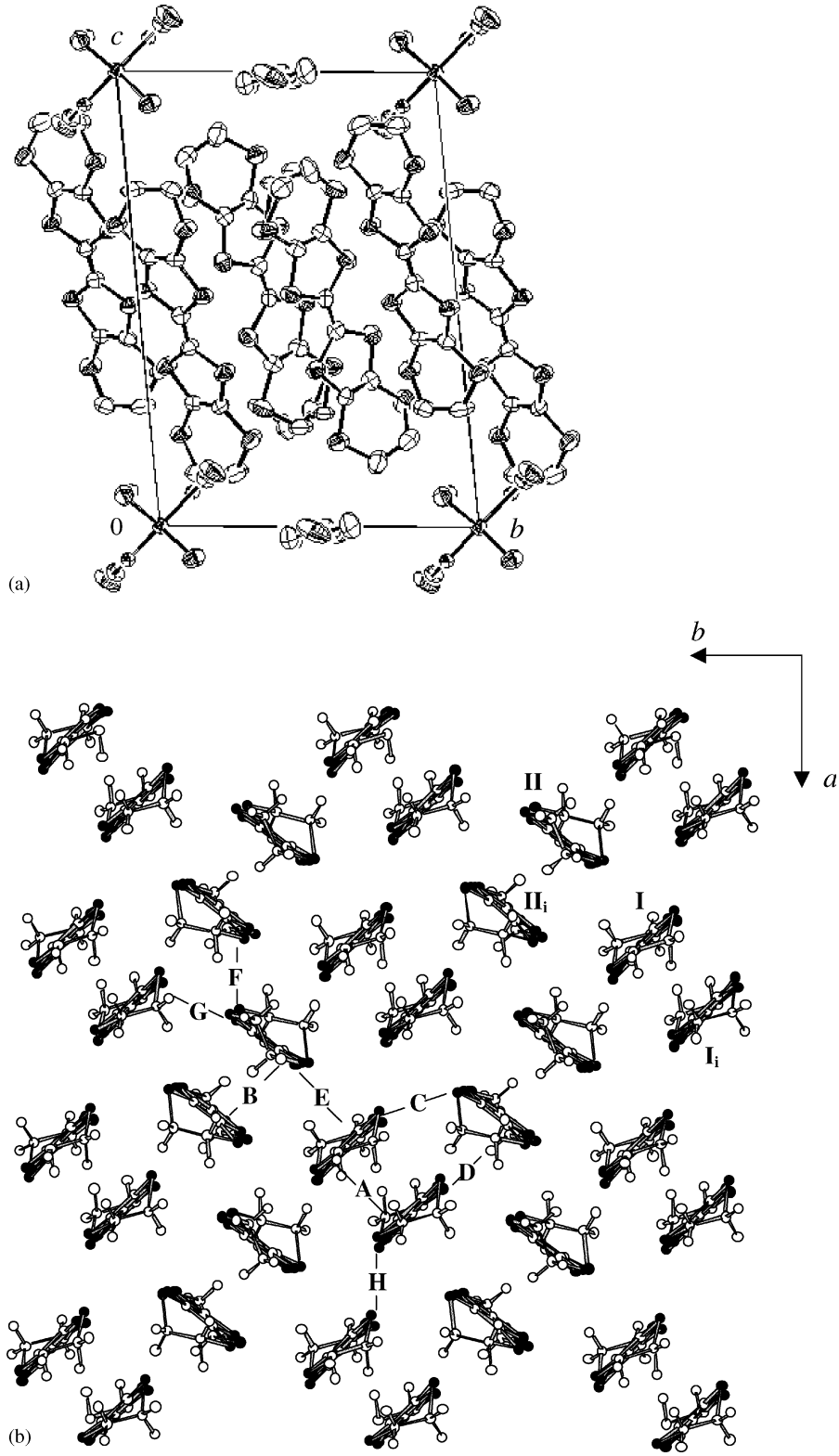

FIG. 1. Crystal structure of κ-(BEDT-TTF)$_4$[RuNOBr$_5$]·BN (**1**): (a) Structural projection along the *a*-direction, (b) projection of the radical cation layer along the long molecular axis in which the different donor···donor interactions are labeled.

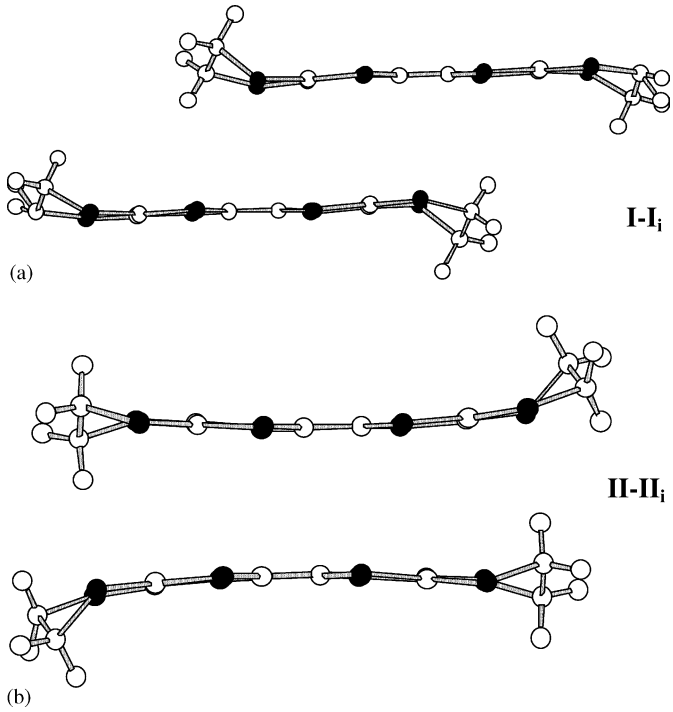

FIG. 2. Side and top views of the overlap modes for the two different donor···donor dimeric units in κ-(BEDT-TTF)$_4$[RuNOBr$_5$]·BN (**1**): (a) dimer I–I$_i$ and (b) dimer II–II$_i$.

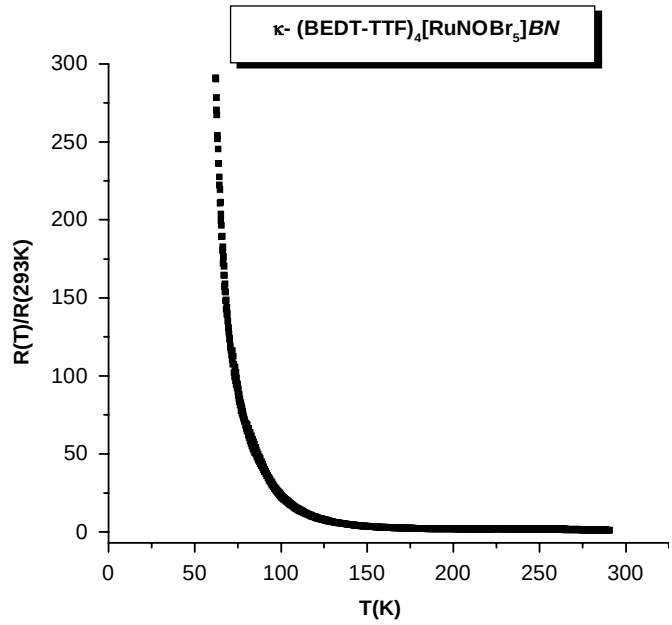

FIG. 3. Temperature dependence of the relative resistivity for a single crystal of κ-(BEDT-TTF)$_4$[RuNOBr$_5$]·BN (**1**).

very similar [33], in the present case one of the two is almost three times larger (see interactions A and B in Table 3). This can be easily understood when the intra-dimer overlap modes are considered. As shown in Fig. 2, there is a large difference in the displacement along the long molecular axis of the donor for the two dimeric units. When the displacement is small, the four pairs of inner sulfur atoms (i.e., those having a strong contribution to the HOMO) are almost on top of each other. The more favorable overlap mode and shorter inter-planar distance (3.46 vs 3.71 Å) lead to quite shorter S···S contacts (cf. interactions B and A in Table 3) and result in a considerably stronger interaction for dimer II–II$_i$. Ultimately, the difference in electronic structure with other κ-phases can thus be traced back to the different kind of interactions of the two BEDT-TTF donors (I and II) with the anion and solvent molecules discussed above.

Coming back to the band structure of Fig. 4, let us note that if it was not for a small overlap in the region of Y and M (or equivalently, S), there would be an energy gap between the two upper bands. Given the stoichiometry of the salt, there must be two holes in the four HOMO bands of Fig. 4. Consequently, the small overlap between the two bands leads to the appearance of hole pockets around Y and electron pockets around M. The size of these pockets is quite small, of the order of 2.5% of the cross section of the first Brillouin zone and thus, **1** should exhibit a typical semimetallic behavior. In principle, the apparent contradiction between the conductivity and band structure results can be explained if we take into account the small number of carriers and the disorder affecting the anions, solvent molecules and donors. In such circumstances, an Anderson-like localization leading to the activated behavior of the conductivity would be quite likely. Alternatively, it

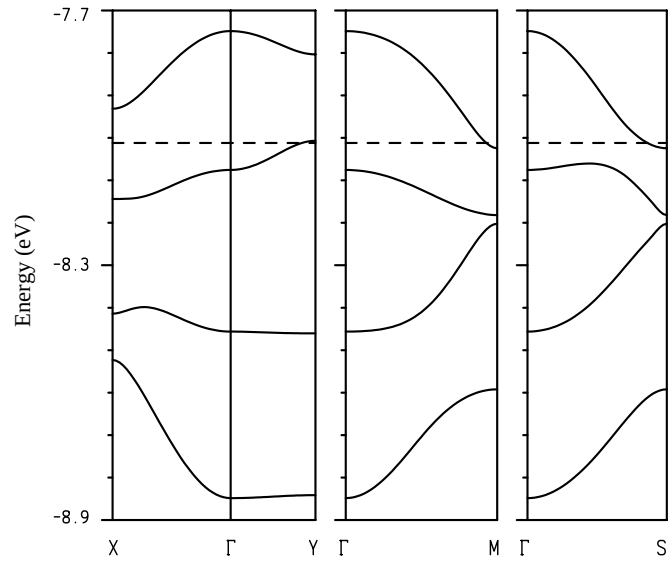

FIG. 4. Band structure for a donor layer of κ-(BEDT-TTF)$_4$[RuNOBr$_5$]·BN (**1**), where the dashed line refers to the Fermi level assuming a metallic filling of the bands: $\Gamma = (0,0)$, $X = (a^*/2,\ 0)$, $Y = (0,\ b^*/2)$, $M = (a^*/2,\ b^*/2)$, and $S = (-a^*/2,\ b^*/2)$.

TABLE 3

Absolute Values of the $\beta_{HOMO-HOMO}$ Intermolecular Interaction Energies (eV) and S···S Distances Shorter than 3.9 Å for the Different Donor···Donor interactions in κ-(BEDT-TTF)$_4$[RuNOBr$_5$]·BN (1)

Interaction type[a]	S···S distances (Å)	$\beta_{HOMO-HOMO}$ (eV)
A	3.753 (×2), 3.896 (×2)	0.2333
B	3.617 (×2), 3.619 (×2)	0.6185
C	3.632, 3.845	0.1140
D	3.715, 3.898	0.0262
E	3.701, 3.834, 3.839	0.1206
F	3.695 (×2), 3.848	0.1989
G	3.482, 3.607, 3.625, 3.690, 3.840	0.0195
H	3.489 (×2), 3.792 (×2), 3.801 (×2)	0.0991

[a] See Fig. 1b for labeling.

could be thought that some computational inaccuracy (either due to the computational details themselves or to some structural parameter which as a consequence of the disorder was not determined precisely enough) could be at the origin of the contradiction. However, a study of the nature of the two upper bands in Fig. 4 suggests that neither of the two explanations is probably quite correct. The upper band is mostly built from the HOMO of the BEDT-TTF donors leading to very strong interaction (i.e., the participation of the $HOMO_{II}$ amounts to practically 85%). This means that if this upper band is empty (second explanation) or nearly empty (first explanation), the BEDT-TTF donors leading to the stronger and weaker interactions must be considered as $(BEDT\text{-}TTF)^{+}$ and $(BEDT\text{-}TTF)^{0}$, respectively. However, this is in contrast with the already noted structural and electronic similarity between the two BEDT-TTF donors. These results suggest that the band description of the electronic structure of **1** is not appropriate. Most likely, a localized description in which one electron is located in each of the two types of dimers is more appropriate and naturally explains the activated conductivity as well as the similarity in the two donors.

It is worth noting that the crystal structure of **1** reminds very much that of κ-$(BEDT\text{-}TTF)_4PtCl_6\cdot BN$, which undergoes a first-order transition at 250 K [35–37]. Probably, the crystals of **1** can also have some phase transition at high temperatures. Indeed, our preliminary results concerning the heating of the samples show that there is a drastic change in the conductivity of the crystals at around 345 K. A high-temperature X-ray study is needed in order to confirm our assumption of a possible phase transition.

According to X-ray diffraction work (rotation and Weissenberg photographs) the radical cation salt **3** is isostructural to **1**. Unfortunately, it was not possible to find a single crystal of good enough quality to carry out the complete structural determination.

3.2. δ-(BEDT-TTF)$_4$[RuNOCl$_5$]$_{1.33}$ (**2**) and δ-(BEDT-TTF)$_4$[RuNOBr$_5$]$_x$ ($x\sim1$) (**4**)

Only the average structure could be determined for **2.** The unit-cell parameters are reported in Table 2. Evidence for a commensurate and incommensurate structural modulation was found from the appearance of satellite reflections corresponding to $3a$ and $2.5a$ for **2** and **4**, respectively. Most probably, the structural modulation is related to the anions' position. The satellite reflections had a diffuse character. The complete pattern of intensities for the crystals **2** could be indexed with the primitive triclinic supercell $a' = 20.15(3)$, $b' = 16.48(2)$, $c' = 37.75(3)$ Å, $\alpha' = 71.21(1)$, $\beta' = 90.05(1)$, $\gamma' = 114.23(1)^\circ$, $V = 10700(2)$ Å^3, $Z = 6\{(BEDT\text{-}TTF)_4[RuNOCl_5]_{1.33}\}$ or $8\{\delta\text{-}(BEDT\text{-}TTF)_3[RuNOCl_5]\}$.

Figure 5a shows the crystal structure of **2** viewed along the *a*-axis. The structure is characterized by BEDT-TTF radical cation layers alternating with anion layers along the *c*-direction. The non-symmetrical anions $[RuNOCl_5]^{2-}$ occupy inversion centers. We were unable to unambiguously distinguish the N–O and Cl ligands because they are statistically distributed over two coordination positions. Nevertheless, we could identify the Cl ligands which are *trans* and *cis* with respect to the nitrosyl group. The $[RuNOCl_5]^{2-}$ anion is a slightly disordered octahedron with a *trans*-(Ru–Cl) bond length of 2.357(2) Å and *cis*-(Ru–Cl) bond lengths of 2.384(3) and 2.391(4) Å. These bond lengths are in good agreement with the corresponding values reported for $K_2[RuNOCl_5]$ (i.e., *trans*-(Ru–Cl): 2.359(2) Å and *cis*-$(Ru\text{–}Cl)_{av}$: 2.372(8) Å) [38] as well as for $Na_2[RuNOCl_5]\cdot 6H_2O$ (i.e., *trans*-(Ru–Cl): 2.352(3) Å and *cis*-(Ru–Cl): 2.372–2.393(4)Å) [39]. Note that an average equatorial Ru–Cl distance of 2.381(2) Å was found in the radical cation salt $(BETS)_2[RuNOCl_5]$ [20].

The radical cation layer is shown in Fig. 5b. The layer is of the δ-type and built from BEDT-TTF stacks running along *b*. The molecular planes of the donors within the stacks are parallel to each other. However, the long molecular axes are not parallel but rotated with respect to each other about a normal to the plane. According to the stoichiometry, the nature of the bond lengths and the angle distribution, the donors should correspond to $(BEDT\text{-}TTF)^{0.67+}$. Indeed, the central C–C bond length (1.369(7) Å) is very close to the average value of the corresponding bond (1.370(5) Å) in the stable organic metal based on BEDT-TTF and the doubly charged $(CuCl_4)^{2-}$ anion, $(BEDT\text{-}TTF)_3CuCl_4H_2O$ (40).

The calculated band structure for the donor layers of **2** is shown in Fig. 6a and the absolute values of the $\beta_{HOMO-HOMO}$ interaction energies (34) are reported in

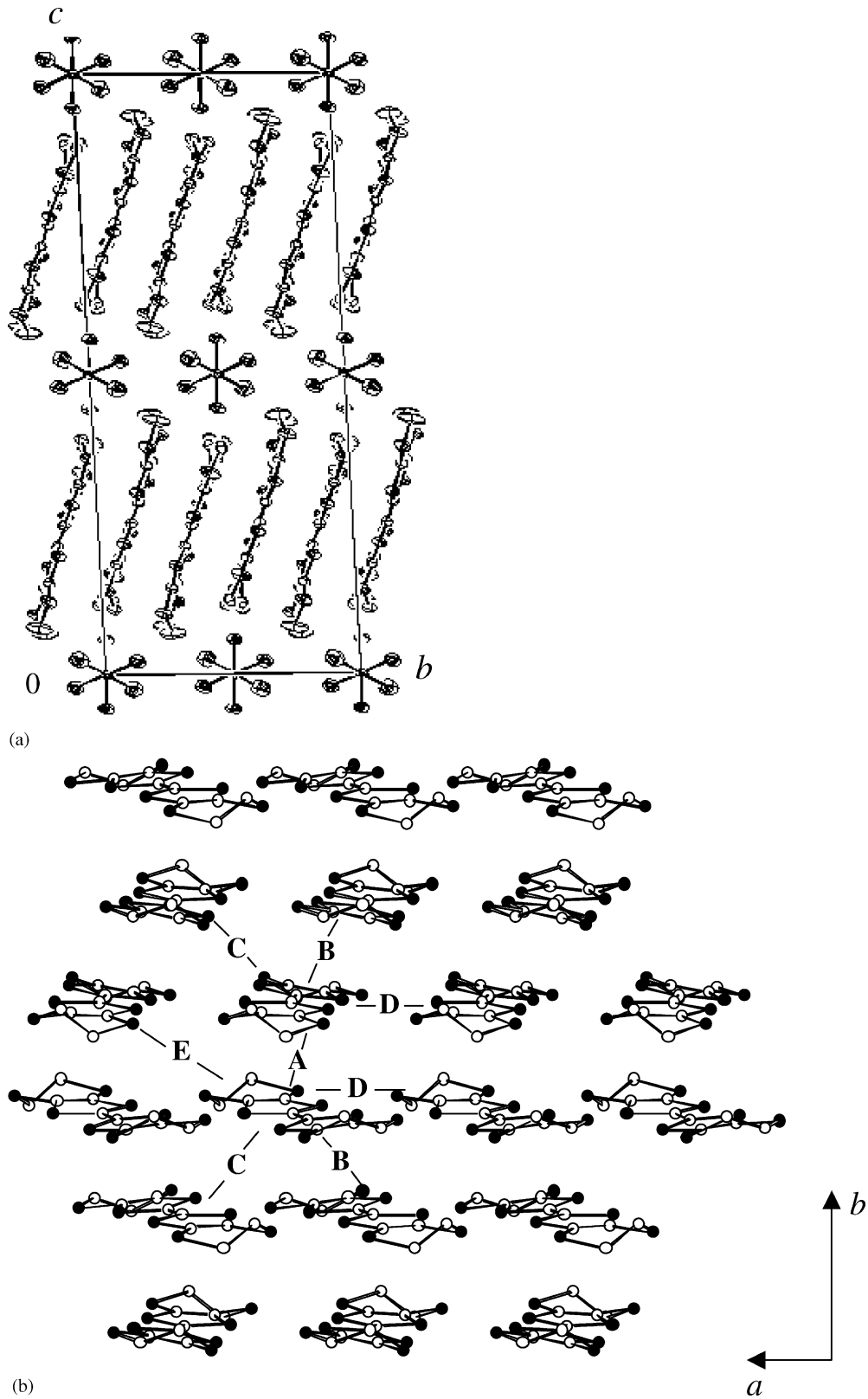

FIG. 5. Crystal structure of δ-(BEDT-TTF)$_4$[RuNOCl$_5$]$_{1.33}$ (**2**): (a) structural projection along the *a*-direction, (b) projection of the radical cation layer showing the different donor···donor interactions.

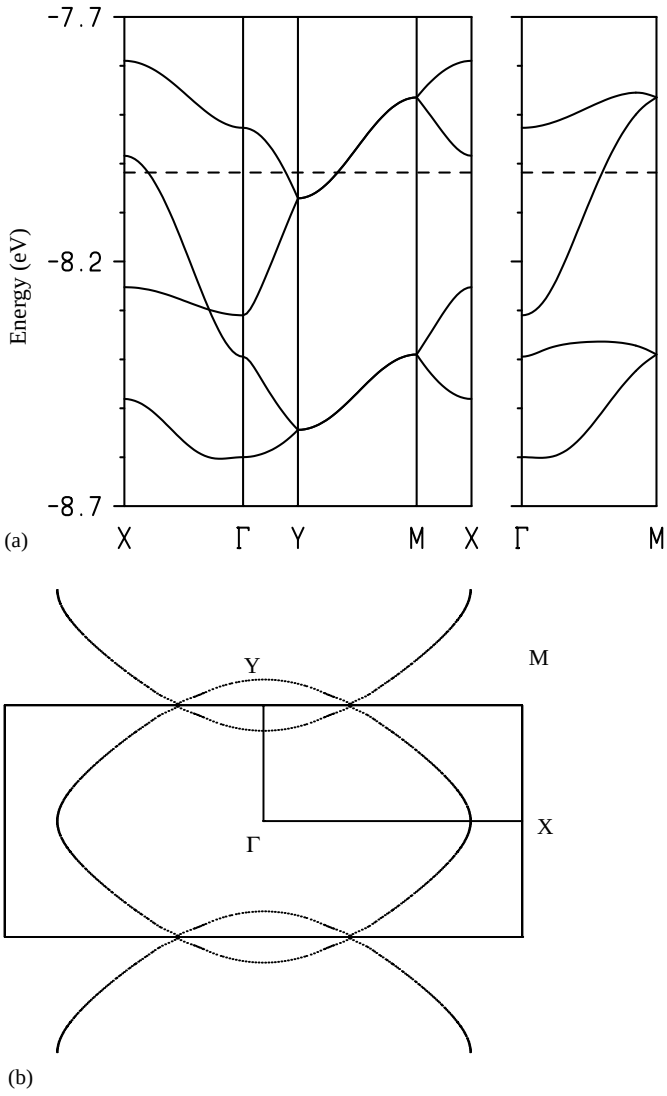

FIG. 6. (a) Band structure and (b) Fermi surface calculated for a donor layer of δ-(BEDT-TTF)$_4$[RuNOCl$_5$]$_{1.33}$ (**2**). The dashed line in (a) refers to the Fermi level and $\Gamma = (0, 0)$, $X = (a^*/2, 0)$, $Y = (0, b^*/2)$ and $M = (a^*/2, b^*/2)$.

Table 4. The repeat unit of the layer contains four donor molecules and consequently, near the Fermi level there are four bands mainly built from the HOMO of the donors. According to the average charge of the donors ($+2/3$), the four HOMO bands must contain 2.66 holes leading to the partial filling of the two upper bands. The dispersion of these partially filled bands is comparable to those of other metallic δ-type BEDT-TTF salts calculated with the same method and, consequently, **2** is predicted to be metallic. The calculated Fermi surface is shown in Fig. 6b and can be described as a series of superposed rounded rhombuses. The area of the full rounded rhombus is determined by the stoichiometry of the salt and is 66% of the cross-sectional area of the first Brillouin zone, whereas the area of the small overlapping region is 5.2%. Thus, both the crystal and electronic structure of this radical cation salt are suggestive of a two-dimensional (2D) organic metal. This can be rationalized on the basis of the $\beta_{HOMO-HOMO}$ interaction energies of Table 4. From the viewpoint of the HOMO$\cdots$HOMO interactions, the donor layers of **2** can be described as a series of parallel chains of twisted dimers (interactions $\cdots$A$\cdots$C$\cdots$A$\cdots$C$\cdots$) interacting considerably through the side-by-side interactions D and to a lesser extent through interactions B and E. Thus, a 2D metallic behavior is expected for **2**.

TABLE 4

Absolute Values of the $\beta_{HOMO-HOMO}$ Intermolecular Interaction Energies (eV) and S$\cdots$S Distances Shorter than 3.9 Å for the Different Donor$\cdots$Donor Interactions in δ-(BEDT-TTF)$_4$[RuNOCl$_5$]$_{1.33}$ (2)

Interaction type[a]	S$\cdots$S distances (Å)	$\beta_{HOMO-HOMO}$ (eV)
A	3.791 ($\times$2), 3.818, 3.865	0.2468
B	3.741 ($\times$2)	0.0718
C	3.697 ($\times$2), 3.769 ($\times$2), 3.863 ($\times$2)	0.2828
D	3.463, 3.490, 3.555 ($\times$2), 3.860	0.1155
E	3.962[b]	0.0492

[a] See Fig. 5b for labelling.
[b] Shortest S$\cdots$S contact.

Regarding salt **4**, on the basis of the analysis of single crystal rotation and Weissenberg photographs, it was found that it is isostructural with **2**, although it has a different structural modulation. Unfortunately, we could not determine the complete crystal structure of **4**. However, the donor-to-anion ratio was determined to be approximately 4:1 on the basis of some crystallochemical considerations taking into account the size of the $[RuNOCl_5]^{2-}$ and $[RuNOBr_5]^{2-}$ anions, their commensurability with the radical cation building block, and the different types of structural modulation.

The normalized resistivity for single crystals of **2** and **4** in the *ab* plane is shown in Fig. 7. The resistivity of δ-(BEDT-TTF)$_4$[RuNOCl$_5$]$_{1.33}$ very slightly grows down to $\sim$50 K ($E_a \cong 0.006$ eV) and then begins to increase sharply (metal-to-insulator transition). It was also found that the room conductivity and the R vs T curve measured along the *a*- and *b*-axis are very similar. Thus, the conductivity in the *ab* plane of δ-(BEDT-TTF)$_4$[RuNOCl$_5$]$_{1.33}$ is practically isotropic. In the case of δ-(BEDT-TTF)$_4$[RuNOBr$_5$]$_x$, a sharp increase of the resistivity occurs at a higher temperature ($\sim$80 K) and the resistivity grows in a steeper way down to 80 K ($E_a \cong 0.02$ eV).

These results bring to the forefront two questions. First, why these salts having 2D conducting layers exhibit an M–I

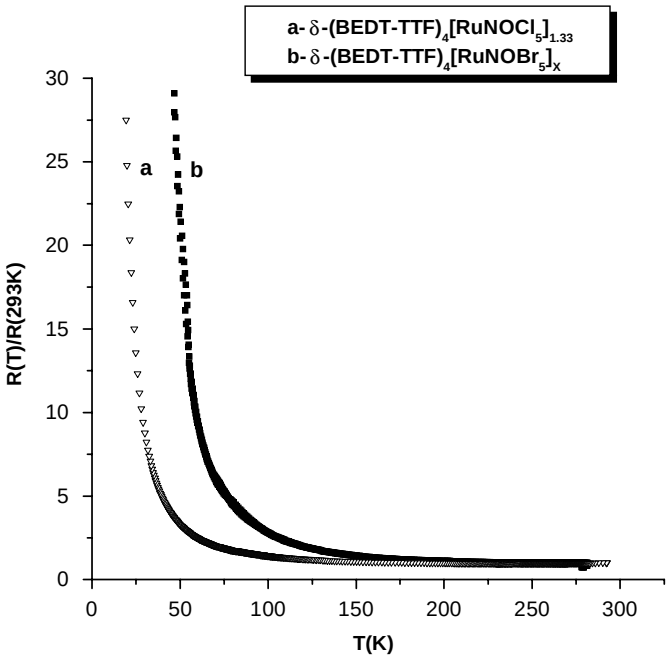

FIG. 7. Temperature dependence of the relative resistivity for a single crystal of δ-(BEDT-TTF)$_4$[RuNOCl$_5$]$_{1.33}$ (**3**) and δ-(BEDT-TTF)$_4$[RuNOBr$_5$]$_x$ ($x \sim 1$) (**4**).

transition? Second, what is the reason for the difference in transition temperatures? A considerable number of radical cation salts with a δ-type packing of the conducting layer are presently known [41]. They exhibit different electrical behaviors which range from metallic to insulating. Only two of them, (BEDT-TTF)$_4$Cl$_2 \cdot 4$H$_2$O [42] and (BEDT-TTF)$_2$Br $\cdot 3$H$_2$O [43], show metallic behavior down to very low temperatures (20 and 4 K, respectively). Some of them, like (BEDT-TTF)$_4$Cl$_2 \cdot 6$H$_2$O (44), (BEDT-TTF)$_2$BrC$_2$H$_4$(OH)$_2$ [45] and δ-(BEDT-TTF)$_2$PF$_6$ [46] exhibit M–I transitions (at 150, 196 and 297 K, respectively). In all δ-salts, the conducting layer is formed by the BEDT-TTF stacks, which run along the direction with a lattice parameter of 14.854–14.993 Å (in our case the *a*-direction), whereas the main short interstack S$\cdots$S contacts occur in the transverse direction with a lattice parameter of 6.607–6.684 Å (in our case the *b*-direction). According to several band structure calculations, these salts are considered to be organic quasi-1D metals with a maximum conductivity along the short inter-stack direction [41]. On the basis of this observation, a unified view of the electronic structure of the δ-type phases, in which the metal-insulator transitions result from a Fermi surface instability due to nesting of the Fermi surface, was suggested [41]. However, the present work casts some doubts on the generality of such proposal. The Fermi surface of Fig. 6 clearly shows that this is not the case for δ-(BEDT-TTF)$_4$[RuNOCl$_5$]$_{1.33}$ because the Fermi surface does not exhibit a nesting vector which could justify an M–I transition. This Fermi surface agrees very well with the already discussed isotropic behavior of the conductivity within the *ab* plane. Let us remind that 2D Fermi surfaces have also been reported for δ-(BEDT-TTF)$_2$AuI$_2$ [47, 48] and (BEDT-TTF)$_2$Br $\cdot 3$H$_2$O [43]. In addition, let us point that the modulation for **2** was already observed at temperatures well above the M–I transition so that it must originate from a different phenomenon than that leading to the loss of the metallic properties. Presumably, the presence of disorder and/or the different periodicity of the anions and the donor arrangement must be related to the M–I transitions at around 50 K (**2**) and 80 K (**4**). However, the way in which the modulation of the anion sublattice can influence the behavior of the conducting electrons (in the presence of disorder) is not at all clear at the present time. The agreement between the conductivity and band structure results clearly validates the Fermi surface of Fig. 6 and suggests that the previously proposed 2D Fermi surfaces for several δ-phases must not necessarily be an artifact due to the overestimation of the interactions along the stacking axis (here the *a*-direction), as previously suggested (41). In any case, our results clearly rule out that nesting in a pseudo-1D Fermi surface is the origin of the M–I transition for **2**.

With respect to the second question, let us note that even if some kind of chemical pressure effect could be proposed as being at the origin of the different M–I temperatures, it should be taken into account that the main structural building block of these salts, (BEDT-TTF)$_4$, has a different charge for the two salts, $+\frac{2}{3}$ and $+\frac{1}{2}$ for **2** and **4**, respectively. In the absence of a complete crystal structure for **4**, we have estimated the hypothetical Fermi surface assuming that a rigid band scheme works for the two isostructural salts **2** and **4**. The different filling leads also to a different Fermi surface because now, as it can be easily understood from Fig. 6a, the Fermi level does not cut the $\Gamma - X$ direction anymore. Thus, the Fermi surface is not made from overlapping rounded rhombuses but from two pairs of open and warped lines parallel to the a^*-direction. Even with all the reservations by which such a Fermi surface should be taken, this result suggests that the two salts could be more different from the electronic than from the structural viewpoints. Let us remind that the two salts have also different types of structural modulation. Without a better knowledge of both the structure of **4** and the influence of the modulation over the conducting electrons in these δ-salts, an answer to the second question above would be premature.

In conclusion, the results concerning the new δ-type salts reported here suggest that we are still far from a sound understanding of the structural and physical behavior of this large class of organic conductors. Further work along this line is certainly needed.

ACKNOWLEDGMENTS

The authors are grateful to Dr. T.M. Buslaeva from Moscow State Academy of Fine Chemical Technology for the supply of mononitrosyl ruthenium complexes for the synthesis of BEDT-TTF salts. This work was supported by an INTAS Grant (Project 00-0651), the Russian Foundation for Basic Research (Projects 00-03-32576 and 02-02-17063), DGI-Spain (Project BFM2000-1312-C02-01), Generalitat de Catalunya (1999 SGR 207), and a joint grant of the Russian Foundation for Basic Research and CNRS (Project 00-03-22000 PICS).

REFERENCES

1. M. Kurmoo, A. W. Graham, P. Day, S. J. Coles, M. B. Hursthouse, J. L. Caulfield, J. Singleton, F. L. Pratt, W. Hayes, L. Ducasse, and P. Guionneau, *J. Am. Chem. Soc.* **117,** 12209 (1995).
2. L. Brossard, R. Clerac, C. Coulon, M. Tokumoto, T. Ziman, D. K. Petrov, V. N. Laukhin, M. J. Naughton, A. Audouard, F. Goze, A. Kobayashi, H. Kobayashi, and P. Cassoux, *Eur. Phys. J. B* **1,** 439 (1998).
3. H. Kobayashi, A. Kobayashi, and P. Cassoux, *Chem. Soc. Rev.* **29,** 325 (2000).
4. E. Coronado, J. R. Galan-Mascaros, C. J. Gomez-Garcia, and V. Laukhin, *Nature* 447 (2000).
5. P. G. Lacroix, R. Clément, K. Nakatani, J. Zyss, and I. Ledoux, *Science* **263,** 658 (1994).
6. S. Bénard, P. Yu, T. Coradin, E. Rivière, K. Nakatani, and R. Clément, *Adv. Mater.* **9,** 981 (1997).
7. K. Sutter, J. Hulliger, and P. Günter, *Solid State Commun.* **74,** 867 (1990).
8. P. G. Lacroix and K. Nakatani, *Adv. Mater.* **9,** 1105 (1997).
9. S. Bénard, E. Rivière, P. Yu, K. Nakatani, and J. F. Delouis, *Chem. Mater.* **13,** 159 (2001).
10. L. Kushch, L. Buravov, V. Tkacheva, E. Yagubskii, L. Zorina, S. Khasanov, and R. Shibaeva, *Synth. Met.* **102,** 1646 (1999).
11. M. Gener, E. Canadell, S. S. Khasanov, L. V. Zorina, R. P. Shibaeva, L. A. Kushch, and E. B. Yagubskii, *Solid State Commun.* **111,** 329 (1999).
12. S. S. Khasanov, L. V. Zorina, and R. P. Shibaeva, *Russ. J. Coord. Chem.* **27,** 259 (2001).
13. L. V. Zorina, S. S. Khasanov, R. P. Shibaeva, M. Gener, R. Rousseau, E. Canadell, L. A. Kushch, E. B. Yagubskii, O. O. Drozdova, and K. Yakushi, *J. Mater. Chem.* **10,** 2017 (2000).
14. I. Yu. Shevyakova, L. I. Buravov, L. A. Kushch, E. B. Yagubskii, S. S. Khasanov, L. V. Zorina, R. P. Shibaeva, N. V. Drichko, and I. Oleinischak, *Russ. J. Coord. Chem.*, in press.
15. R. P. Shibaeva, E. B. Yagubskii, E. Canadell, S. S. Khasanov, L. V. Zorina, L. A. Kushch, T. G. Prokhorova, I. Yu. Shevyakova, L. I. Buravov, V. A. Tkacheva, and M. Gener, *Synth. Met.*, in press.
16. L. V. Zorina, M. Gener, S. S. Khasanov, R. P. Shibaeva, E. Canadell, L. A. Kushch, and E. B. Yagubskii, *Synth. Met.* **128,** 325 (2002).
17. M. Clemente-León, E. Coronado, J. R. Galán-Mascarós, C. Giménez-Saiz, C. J. Gómez-García, and J. M. Fabre, *Synth. Met.* **103,** 2279 (1999).
18. M. Clemente-León, E. Coronado, J. R. Galán-Mascarós, C. J. Gómez-García, and E. Canadell, *Inorg. Chem.* **39,** 5394 (2000).
19. M. Clemente-León, E. Coronado, J. R. Galán-Mascarós, C. Giménez-Saiz, C. J. Gómez-García, E. Ribera, J. Vidal-Gancedo, C. Rovira, E. Canadell, and V. Laukhin, *Inorg. Chem.* **40,** 3526 (2001).
20. M.-E. Sanchez, M.-L. Doublet, C. Faulmann, I. Malfant, P. Cassoux, L. A. Kushch, and E. B. Yagubskii, *Eur. J. Inorg. Chem.* 2797 (2001).
21. T. Woike, W. Krasser, P. Bechthold, and S. Haussühl, *Phys. Rev. Lett.* **53,** 1767 (1984).
22. H. Zöllner, T. Woike, W. Krasser, and S. Haussühl, *Z. Kristallogr.* **188,** 139 (1989).
23. T. Woike, H. Zöllner, W. Krasser, and S. Haussühl, *Solid State Commun.* **73,** 149 (1990).
24. T. Woike and S. Haussühl, *Solid State Commun.* **86,** 333 (1993).
25. M. R. Pressprich, M. A. White, V. Vekhter, and P. Coppens, *J. Am. Chem. Soc.* **116,** 5233 (1994).
26. M. D. Carducci, M. R. Pressprich, and P. Coppens, *J. Am. Chem. Soc.* **119,** 2669 (1997).
27. V. I. Andrianov, "AREN-88. The System of Programs for Solving and Refinement of Crystal Structures." Institute of Crystallography AN SSSR, Moscow, 1988.
28. G. M. Sheldrick, "SHELXL-93, Program for the Refinement of Crystal Structure." Göttingen University, Germany, 1993.
29. M.-H. Whangbo and R. Hoffmann, *J. Am. Chem. Soc.* **100,** 6093 (1978).
30. J. Ammeter, H.-B. Bürgi, J. Thibeault, and R. Hoffmann, *J. Am. Chem. Soc.* **100,** 3686 (1978).
31. A. Pénicaud, K. Boubekeur, P. Batail, E. Canadell, P. Auban-Senzier, and D. Jérome, *J. Am. Chem. Soc.* **115,** 4101 (1993).
32. Y. N. Mikhailov, A. S. Kanishcheva, and A. A. Svetlov, *Zh. Neorg. Khim.* **34,** 2803 (1989).
33. D. Jung, M. Evain, J. J. Novoa, M.-H. Whangbo, M. A. Beno, A. M. Kini, A. J. Schultz, J. M. Williams, and P. J. Nigrey, *Inorg. Chem.* **28,** 4516 (1989).
34. M.-H. Whangbo, J. M. Williams, P. C. W. Leung, M. A. Beno, T. J. Emge, and H. H. Wang, *Inorg. Chem.* **24,** 3500 (1985).
35. A. A. Galimzyanov, A. A. Ignat'ev, N. D. Kushch, V. N. Laukhin, M. K. Makova, V. A. Merzhanov, L. P. Rozenberg, R.P. Shibaeva, and E. B. Yagubskii, *Synth. Met.* **33,** 81 (1989).
36. V. E. Korotkov, V. N. Molchanov, and R. P. Shibaeva, *Sov. Phys. Crystallogr.* **37,** 776 (1992).
37. M.-L. Doublet, E. Canadell, and R. P. Shibaeva, *J. Phys. I France* **4,** 1479 (1994).
38. J. T. Veal and D. J. Hodgson, *Acta Crystallogr. B* **28,** 3525 (1972).
39. V. A. Emel'yanov, S. A. Gromilov, I. A. Baidina, A. V. Virovets, A. V. Belyaev, and V. A. Logvinenko, *Russ. J. Strukt. Khim.* **40,** 1091 (1999).
40. R. P. Shibaeva, V. E. Korotkov, and L. P. Rozenberg, *Sov. Phys. Crystallogr.* **36,** 820 (1991).
41. T. Mori, *Bull. Chem. Soc. Jpn.* **72,** 2011 (1999).
42. R. P. Shibaeva, L. P. Rozenberg, A. F. Shestakov, and T. A. Khannanova, *Russ. J. Strukt. Khim.* **32,** 98 (1991).
43. M. Luo, T. Ishida, A. Kobayashi, and T. Nogami, *Synth. Met.* **96,** 97 (1998).
44. G. Bravic, D. Chasseau, J. Gaultier, M. J. Rosseinsky, M. Kurmoo, P. Day, and A. Filhol, *Synth. Met.* **42,** 2035 (1991).
45. N. P. Karpova, S. V. Konovalikhin, O. A. Dyachenko, R. N. Lyubovskaya, and E. I. Zhilyaeva, *Acta Crystallogr. C* **48,** 62 (1992).
46. H. Kobayashi, T. Mori, R. Kato, A. Kobayashi, Y. Sasaki, G. Saito, and H. Inokuchi, *Chem. Lett.* 581 (1983).
47. A. Kobayashi, R. Kato, H. Kobayashi, M. Tokumoto, H. Anzai, and T. Ishiguro, *Chem. Lett.* 1117 (1986).
48. M.-H. Whangbo, M. Evain, M. A. Beno, H. H. Wang, K. S. Webb, and J. M. Williams, *Solid State Commun.* **68,** 421 (1988).